Al and B ion-implantations in 6H- and 3C-SiC

Mulpuri V. Rao, Peter Griffiths, O. W. Holland, G. Kelner, J. A. Freitas Jr., David S. Simons, P. H. Chi, and M. Ghezzo

Citation: Journal of Applied Physics **77**, 2479 (1995); doi: 10.1063/1.358776
View online: http://dx.doi.org/10.1063/1.358776
View Table of Contents: http://scitation.aip.org/content/aip/journal/jap/77/6?ver=pdfcov
Published by the AIP Publishing

Al and B ion-implantations in 6H- and 3C-SiC

Mulpuri V. Rao and Peter Griffiths
Department of Electrical and Computer Engineering, George Mason University, Fairfax, Virginia 22030

O. W. Holland
Oak Ridge National Laboratory, Oak Ridge, Tennessee 37831

G. Kelner and J. A. Freitas, Jr.[a)]
Naval Research Laboratory, Washington, D.C. 20375

David S. Simons and P. H. Chi
National Institute of Standards and Technology, Gaithersburg, Maryland 20899

M. Ghezzo
GE Corporate Research and Development, Schenectady, New York 12301

(Received 27 July 1994; accepted for publication 28 November 1994)

Low (keV) and high (MeV) energy Al and B implants were performed into n-type 6H- and 3C-SiC at both room temperature and 850 °C. The material was annealed at 1100, 1200, or 1400 °C for 10 min and characterized by secondary ion mass spectrometry, Rutherford backscattering (RBS), photoluminescence, Hall and capacitance-voltage measurement techniques. For both Al and B implants, the implant species was gettered at 0.7 R_p (where R_p is the projected range) in samples implanted at 850 °C and annealed at 1400 °C. In the samples that were amorphized by the room temperature implantation, a distinct damage peak remained in the RBS spectrum even after 1400 °C annealing. For the samples implanted at 850 °C, which were not amorphized, the damage peak disappeared after 1400 °C annealing. P-type conduction is observed only in samples implanted by Al at 850 °C and annealed at 1400 °C in Ar, with 1% dopant electrical activation. © *1995 American Institute of Physics.*

I. INTRODUCTION

SiC, whose polytypes possess a range of wide band gaps[1] with a higher saturated electron drift velocity, junction breakdown electric field, and thermal conductivity, and a lower dielectric constant compared to Si and GaAs, is emerging as a potential candidate for high-temperature, high-voltage, microwave, blue light source, and UV detector device applications.[2–4] Currently, doping of SiC devices is achieved mostly *in situ* during epitaxial growth. This approach does not offer planar selective area doping which is crucial for making economical SiC integrated circuits. As opposed to Si technology, thermal diffusion cannot be used due to a very low diffusion coefficient of the impurities at temperatures where dielectric masking layers can be used for selective area doping.[2] This leaves ion-implantation as the only viable selective area doping technique for SiC device production. The recent availability of reasonably good quality bulk 6H- and 4H-SiC substrates from vendors makes ion implantation an attractive doping technique for making SiC devices.

In the past there were several studies[5–22] of the ion implantation doping of SiC. In these studies the implanted material was not thoroughly characterized so definitive statements about the thermal stability of the implant and structural, electronic and p-n junction properties of the implanted layers were not possible. In the previous studies implants were mostly performed either at room temperature or at temperatures <600 °C which resulted in heavy lattice damage. This requires very high post-implant annealing temperatures (>1600 °C) which are prohibitive for reproducible and high-yield device production due to thermal pitting generated on the surface of the samples. In these studies the emphasis was given to either structural or p-n junction properties rather than to a more comprehensive evaluation of the implanted layer. This warrants a more detailed study of the ion implantation in SiC especially with the recent availability of good quality substrates.

In this work we have concentrated on the implantation of acceptor species (Al and B) in 6H- and 3C-SiC at both room temperature and at 850 °C. The implanted material was evaluated for thermal stability of the implants, lattice perfection, and the electrical activation of the dopant. The Al is a preferred acceptor in SiC due to its lower activation energy (0.24 eV) compared to other acceptors (0.33–0.7 eV for B and 0.33 eV for Ga),[23] which results in less carrier freeze-out at room temperature, whereas B with its low atomic weight offers greater penetration depth than the other acceptors. In this work implantations were done at 200 keV, 850 keV, 1.2 MeV, and 2 MeV. MeV energy implantations are required to make devices with thick or buried doped layers, for example, wells of complementary field effect transistor (FET) devices. The inherent planarity offered by selective area ion implantation makes it an attractive technique for fabrication of integrated circuits and device arrays such as UV detector arrays.

II. EXPERIMENT

In this work we have used three types of SiC acquired from Cree Research:[51] a bulk n-type on-axis (1000)-oriented

[a)]SFA Inc., Landover, MD 20789.

 0021-8979/95/77(6)/2479/7/$6.00

Si-faced 6H-SiC wafer with a carrier concentration (n) of 6×10^{17} cm^{-3}; a 4 μm thick epitaxial layer with n=1.5×10^{15} cm^{-3} grown on an off-axis (1000)-oriented 6H-SiC (n=3.3×10^{17} cm^{-3}) wafer; and a 3.1 μm thick 3C epitaxial layer with n=2.8×10^{16} cm^{-3} grown on an n-type on-axis (001) Si wafer with a resistivity of 10 Ω-cm. The implantations were done using a high-current, high-energy implanter. Both the Al and B ion beams were produced from elemental source material. The 200 keV energy ion implants were done using a singly ionized species whereas MeV energy range beams were obtained by using ions of higher charge states. The implants were performed either at room temperature (RT) or at an elevated temperature (ET) of 850 °C using a holder which could be resistively heated. During implantation the SiC substrates were tilted 7° off the normal to minimize channeling.

The 6H-SiC samples were annealed at 1100 or 1400 °C and the 3C-SiC samples at 1200 °C. In this study, the anneal time for all samples was 10 min at the stated temperature, since no appreciable changes were observed in the electrical and structural properties of implanted SiC for longer anneal times at a given temperature.[20] The 1100 and 1200 °C anneals were done in standard Si device processing furnaces using SiC-coated tubes and standard quartz boats in a N_2 atmosphere. The 1400 °C anneal was performed in a high temperature ceramic processing furnace in an Ar atmosphere slightly above 1 atm. pressure using a SiC crucible. The SiC crucible has been observed to prevent the deterioration of the SiC sample surface caused by sublimation or etching of Si from the SiC substrates which otherwise frequently occurs at temperatures above 1300 °C.[21] The samples annealed in the N_2 atmosphere were subsequently dipped in dilute HF to remove the nitride layer formed on the sample surface during annealing.

The secondary ion mass spectrometry (SIMS) depth profiles of the ^{27}Al and ^{11}B implants in the as-implanted and annealed samples were obtained using an ion microscope operating with an 8 or 10.5 keV impact energy O_2^+ primary beam. Concentration scales were calibrated according to the stated implant fluences and the depth scales were calibrated by stylus profilometer measurements of each crater. Ion-induced damage in the as-implanted material and residual damage after post-implantation annealing were evaluated by Rutherford back scattering (RBS) techniques. A 2.3 MeV He^{++} beam was used with a standard solid-state detector positioned to detect scattering events at 160°. Ion channeling spectra were acquired along (1000), which was within 4° of the normal in all samples. Kinematical separation due to the mass of the lattice atoms results in scattering at 1.32 MeV from surface Si atoms and 0.6 MeV from surface C. Therefore, the spectral composition over this energy interval consists only of scattering events within the Si sublattice, ranging from the surface (for 1.32 MeV) to a depth of ~1.1 μm (for 0.6 MeV). This allows damage in the Si sublattice over this depth to be determined unambiguously from the spectra data. However, the scattering profiles from C and Si overlap below this range making such a determination impossible. A depth scale is shown at the top of the spectra which correlated the scattering energy with the depth of the event for scattering from the Si lattice atoms. Also, an aligned spectrum from a virgin (non-implanted) crystal, and a random spectrum are shown for comparison purposes in each of the figures containing RBS data.

TABLE I. Range statistics of Al and B ions in 6H-SiC.

Ion	Implant energy (MeV)	Implant temp. (°C)	R_p (μm)	ΔR_p (μm)	γ	β	TRIM-92 R_p (μm)	TRIM-92 ΔR_p (μm)
Al	0.2	RT	0.226	0.070	0.34	7.81	0.219	0.053
	1.2	850	0.956	0.157	−0.55	6.23	1.05	0.130
	2	RT	1.529	0.257	−1.95	5.50	1.41	0.143
B	0.2	850	0.397	0.071	−1.21	6.64	0.410	0.069
	0.85	850	1.058	0.106	−3.05	25.0	1.09	0.097

To evaluate the electrical activation of the dopant, van der Pauw Hall and C-V profiling, on the Schottky junctions formed on the surface of the implanted layer, were used. Before the Al Schottky contacts were deposited, a thin layer of the surface (up to the depth where the SIMS atom concentration is ~1×10^{19} cm^{-3}) was removed by reactive ion etching. This was done to remove the thin n-type layer on the sample surface which was not converted to p-type, either due to a low acceptor activation and/or a higher background n-type carrier concentration compared to the acceptor concentration of the implant profile in that region.

III. RESULTS AND DISCUSSION

A. SIMS

The range (R_p), straggle (ΔR_p), skewness (γ), and kurtosis (β) obtained by analyzing the as-implanted SIMS profiles of the 850 °C or RT implanted Al and B in 6H-SiC are given in Table I. For comparison the R_p and ΔR_p values obtained from TRIM-92[24] PRAL calculations are also included in Table I. In general, the experimental R_p values are close to the corresponding TRIM values. The experimental ΔR_p values are also close to the TRIM values at low ion energies, but at MeV energies the TRIM ΔR_p values are considerably smaller than the corresponding experimental values. In general, for the same implant energy the ΔR_p value for the ET implants is slightly larger than the RT implant value due to a greater amount of channeling that occurs in ET implant compared to the RT implants. The SIMS profiles before and after annealing for 200 keV Al and B implants at 850 °C are shown in Figs. 1(a) and 1(b), respectively. For both Al and B implants, the implant gettering to ~0.7 R_p is observed in samples annealed at 1400 °C. No implant redistribution is observed for 1100 °C annealing. Similar annealing results were observed for higher implant energies. The 0.7 R_p location is where implant damage is maximum.[25,26] For the 850 °C implant, the lattice damage is much below the amorphization level as discussed later in RBS results. For the RT implantation, amorphization of SiC is observed from near the surface to R_p for the fluences selected in this study. For the RT implant a small gettering peak is seen close to R_p as shown in Fig. 1(c) for 200 keV/8×10^{14} cm^{-2} Al. For 850 °C implants the gettering peak formed at ~0.7 R_p acts as an out-diffusion front. For the annealing temperatures used in this study only a

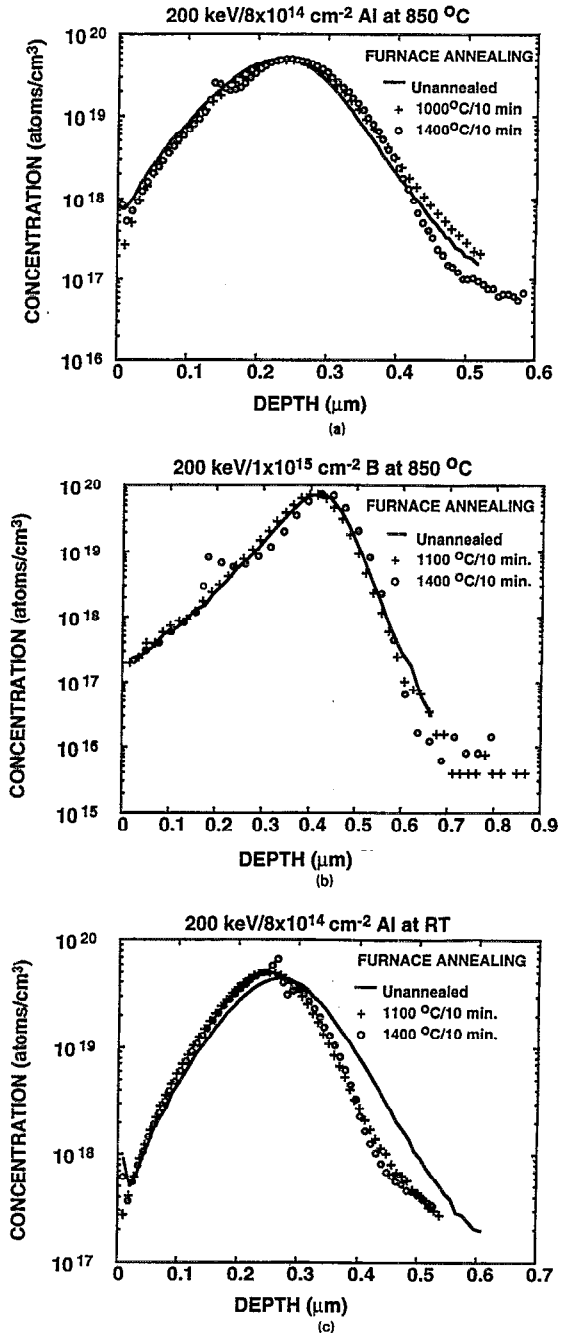

FIG. 1. SIMS implant atom density depth profiles in 6H-SiC before and after annealing for (a) 200 keV/8×10^{14} cm^{-2} Al-implant at 850 °C; (b) 200 keV/1×10^{15} cm^{-2} B-implant at 850 °C; (c) 200 keV/8×10^{14} cm^{-2} Al-implant at room temperature.

slight in-diffusion of the implant is observed. Comparison of Figs. 1(a) and 1(b) reveals that the B redistribution, although small, is more pronounced than that of Al. This probably is due to the smaller atom size of B compared to Al. For 3C-SiC samples, no out-diffusion was observed for the 1200 °C annealing temperature used in this study.

Another explanation for the redistribution of Al and B in SiC is stoichiometric disturbances caused by the implantation.[26,27] Ion implantation in SiC creates a net C and Si vacancy region from the surface to $\sim R_p$ whereas in the region

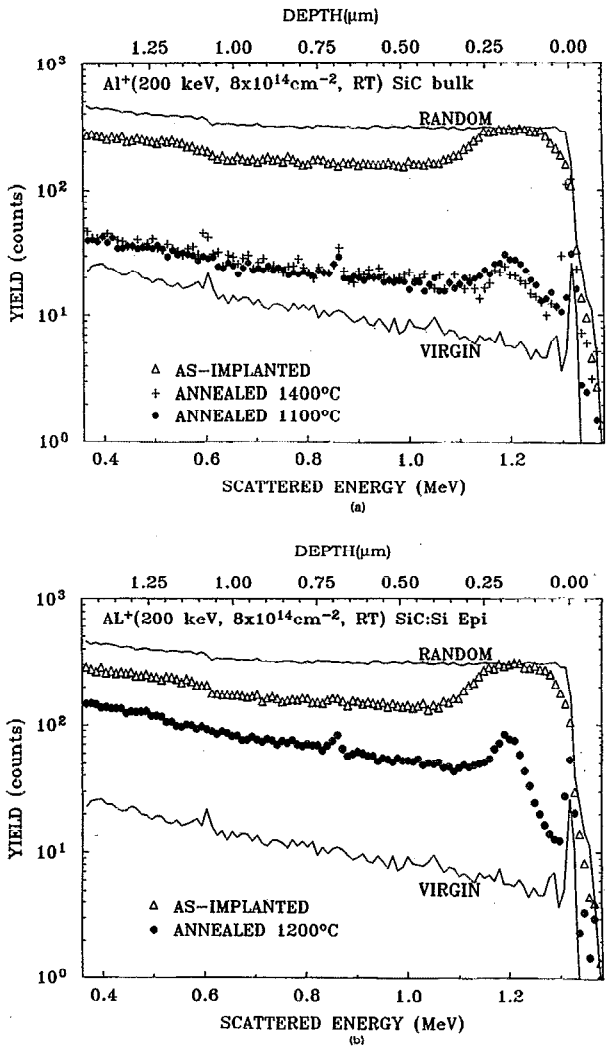

FIG. 2. RBS spectra recorded on room temperature 200 keV/8×10^{14} cm^{-2} Al-implanted (a) bulk 6H-SiC and (b) 3C-SiC, before and after annealing.

deeper than R_p net Si and C interstitials are created.[26,27] During annealing, since the surface region has more lattice vacancies than the bulk, the Al and B atoms move into this region. Based on the atom size, Al is likely to take Si lattice sites and B the C lattice sites. According to the transport equation calculations carried out by Christel and Gibbons,[26] in the surface region, the concentration of C vacancies is more than that of Si. This probably is the reason for the more pronounced diffusion of B than Al.

Addamiano *et al.*[8] and Lucke *et al.*[28] have reported both out- and in- diffusion of Al after 1400 °C/15 min heat treatment for RT implants. Ryu *et al.*[20] have observed out-diffusion of B in B-implanted 3C-SiC for annealing temperatures $\geqslant$1600 °C. Edmond *et al.*[13] have reported out-diffusion of Al in RT Al-implanted 3C-SiC for 1800 °C annealing.

B. RBS

The RBS spectra recorded on RT 200 keV/8×10^{14} cm^{-2} Al-implanted bulk 6H-SiC and 3C-SiC (epilayer grown on Si) are shown in Figs. 2(a) and 2(b), respectively. In both

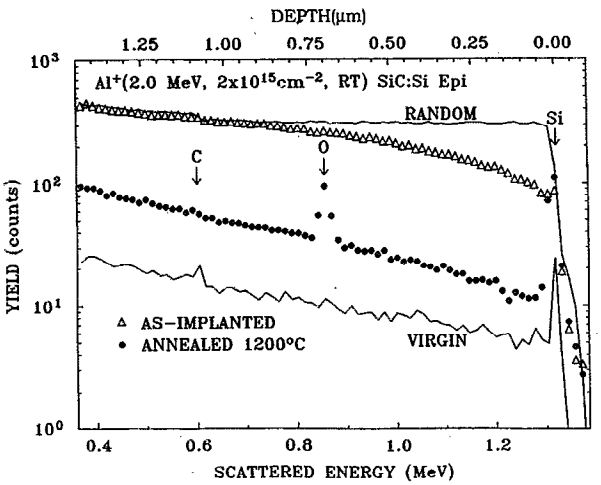

FIG. 3. RBS spectra recorded on room temperature 2 MeV/2×10^{15} cm^{-2} Al-implanted 3C-SiC before and after annealing.

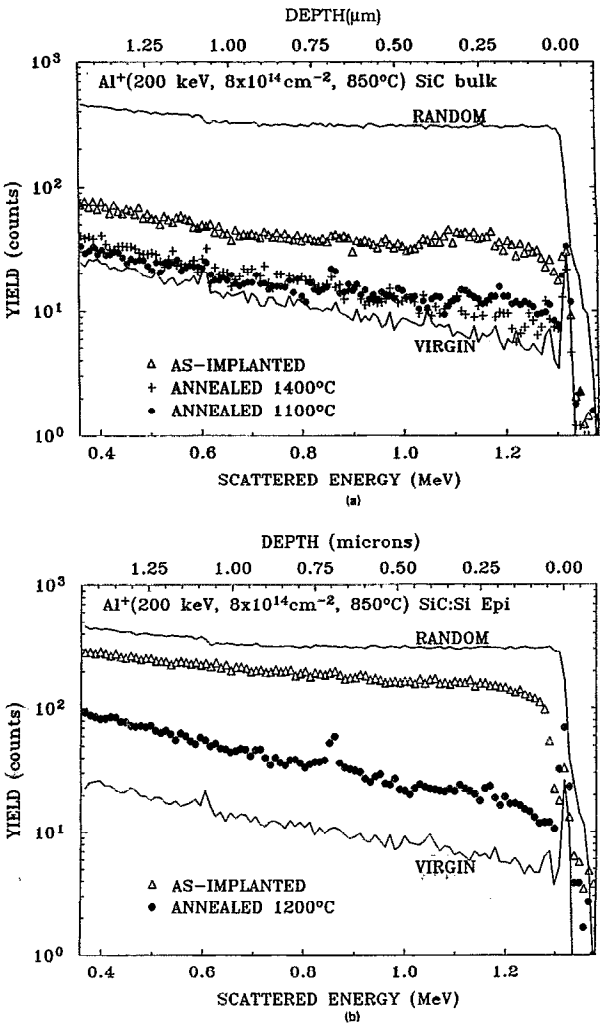

FIG. 4. RBS spectra recorded on elevated temperature (850 °C) 200 keV/8×10^{14} cm^{-2} Al-implanted (a) bulk 6H-SiC, and (b) 3C-SiC, before and after annealing.

samples the aligned spectra from the as-implanted samples almost coincide with the random spectra in the region close to the sample surface indicating near amorphization. In both samples the amorphous layer extends from a depth of 0.08 μm from the surface to a depth of 0.25 μm. For RT 2 MeV/2×10^{15} cm^{-2} Al in 3C-SiC near amorphization occurred below a depth of 0.9 μm, as shown in Fig. 3. Accumulation of displacement damage often causes the implanted layer to be non-crystalline at high doses. Though the threshold displacement energy of SiC is five times greater than for Si,[29] for the doses used in this study either amorphization or near amorphization of SiC is expected for room temperature implantation. Since the doses used in this study are not too high, amorphization is observed only at peak implant damage depth locations (in the vicinity of 0.7 R_p). For higher doses a continuous amorphous layer starting from the surface will be created.

In this study, annealing the samples resulted in lattice recovery for both 6H- and 3C-SiC; but, in the region where the as-implanted material is amorphized, though the amorphization is removed, a distinct damage peak appeared even after 1400 °C annealing. This indicates a substantial amount of residual damage in these RT Al-implanted samples even after annealing.[30,31] The thickness of the damage peak decreases with increasing annealing temperature. The solid-phase epitaxial (SPE) regrowth during annealing seems to occur from crystalline/amorphous interfaces on both sides of the damaged layer. Substantial lattice damage is present over the entire range extending to a depth of >0.87 μm as shown in Fig. 3. In Figs. 2 and 3, for samples annealed at 1100 and 1200 °C, an O peak is observed at an energy of 0.85 MeV. This is due to the formation of a thin oxide layer on the sample surface during open quartz tube furnace annealing for these samples. The oxide layer formed on the sample surface was not removed before RBS measurements, but it was removed before electrical measurements.

The RBS spectra on the 6H- and 3C-SiC samples implanted at 850 °C are shown in Figs. 4(a) and 4(b), respectively, for 200 keV/8×10^{14} cm^{-2} Al. In both samples the aligned yield in the as-implanted material is substantially below the random level. It is clear that the dynamic annealing during elevated temperature implantation prevented amorphization. After 1100 °C annealing, the scattering yield (over the top 0.4 μm) is much reduced indicating some lattice recovery. After 1400 °C, additional annealing is observed [in Fig. 4(a)] as indicated by the low yield which almost coincides with the virgin level at all depths. Similar behavior was observed for an MeV Al implant in 6H-SiC as shown in Fig. 5. Based on the above results, it can be stated that the implant and anneal temperatures are dominant parameters in reducing the implant damage. It was reported[20] that the anneal time is not a dominant parameter in implant damage removal compared to the above two parameters.

For some of the samples annealed at 1400 °C, RBS peaks were observed at the surface. This probably is a result of preferential evaporation of Si at 1400 °C leaving a C-rich disordered surface layer. From Figs. 2(a) and 2(b) it can be seen that the RBS yield in 3C-SiC samples after 1200 °C

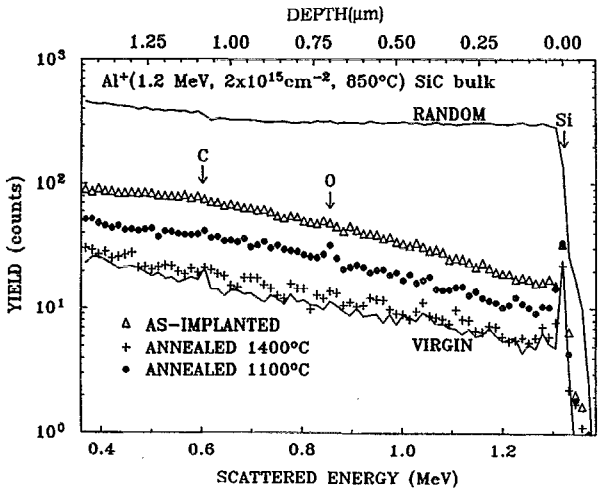

FIG. 5. RBS spectra recorded on elevated temperature (850 °C) 1.2 MeV/ 2×10^{15} cm^{-2} Al-implanted bulk 6H-SiC before and after annealing.

annealing is much more than the yield in 6H-SiC after 1100 °C annealing. The 1200 °C annealing is expected to provide a lower damage yield compared to the 1100 °C annealing. The higher yield in the 3C-SiC epitaxial sample probably is due to strain caused by the lattice mismatch between the 3C-SiC epilayer and the Si substrate.

C. Photoluminescence

Low-temperature photoluminescence (PL) is widely used as a nondestructive technique to evaluate the extent of lattice recovery and implant activation after the post-implantation annealing step in semiconductors. The PL in 3C-SiC before and after 850 °C Al implantation and annealing is shown in Fig. 6. The spectral lines in the energy range 2.35–2.25 eV are assigned to the zero-phonon line and phonon replicas of the four-particle nitrogen bound exciton complexes.[32] N is a well known residual impurity in SiC.[33] The peak at~2.17 eV is known as the W-band.[34,35] All of the remaining peaks in the spectra are attributed to zero-phonon and phonon replicas of defect-related transitions.[32,36] The presence of these defect bands in the as-grown material indicates a high defect content in the material which may have resulted from lattice mismatch between the Si substrate and the 3C-SiC film. In the as-implanted material the PL intensity is very low and only structural-defect-related bands are observed in the spectra indicating lattice damage. After 1200 °C annealing no edge emission is detected. However, the PL spectrum for energies < 2.0 eV is dominated by an intense defect band. The intensity of the defect-related peaks in the annealed material is almost 10 times stronger than in the as-grown material. This indicates incomplete annealing of the lattice damage induced by implantation. This result is in agreement with the RBS measurements. The absence of a N-Al donor-acceptor-pair (DAP) band indicates either very poor or no Al acceptor activation in the material after the 1200 °C annealing.

The PL in as-grown and 850 °C Al-implanted (annealed at 1400 °C) 6H-SiC is shown in Fig. 7. The sharp lines at energies >2.8 eV are attributed to bound exciton transitions

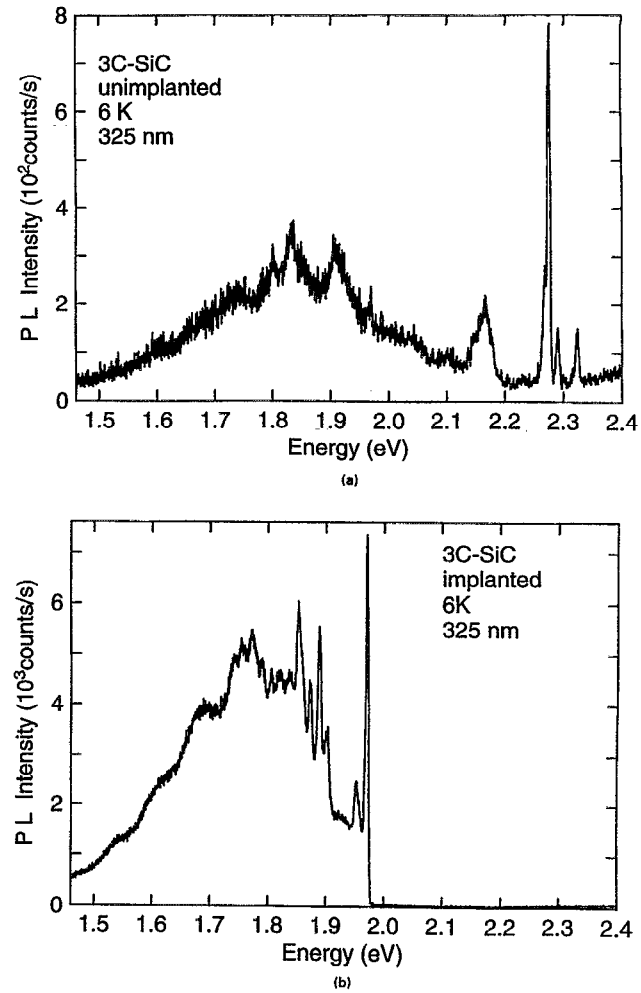

FIG. 6. Photoluminescence in (a) virgin and (b) elevated temperature (850 °C) 200 keV/8×10^{14} cm^{-2} Al-implanted 3C-SiC after 1200 °C/10 min annealing.

involving N donors[33] and to Ti isoelectronic impurities.[33,37,38] The multiple peaks observed in the PL spectra of 6H-SiC result from the three inequivalent sites for the dopant, two cubic and one hexagonal. The peaks measured at energies <2.6 eV are defect-related.[33,37] In the ion implanted material even after 1400 °C annealing the intensity of exciton peaks is relatively weak compared to defect-related peaks. The three most intense peaks at energies <2.63 eV are attributed to thermally stable D_1 centers in which the two peaks not seen in the as-grown material are introduced by ion implantation.[37,39] The peaks at lower energies are phonon contributions of the three sharp defect peaks. Patrick and Choyke[39] have considered the C-Si nearest neighbor divacancy as a possible model for the D_1 center. The DAP-related peaks and their phonon replicas which typically appear in the energy range 2.8 to 2.5 eV in Al-doped 6H-SiC[23] are not observed in the implanted material. This probably is due to either very poor or no electrical activation of Al for the annealing conditions used in this study. Similar PL behavior was observed for B-implanted samples. The compensation

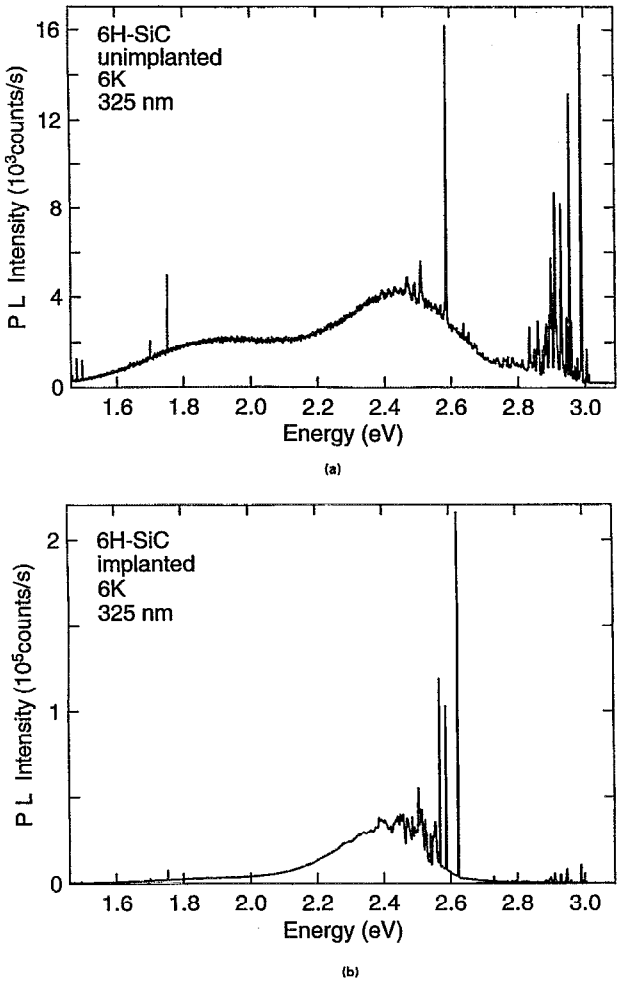

FIG. 7. Photoluminescence in (a) virgin and (b) elevated temperature (850 °C) 200 keV/8×10^{14} cm^{-2} Al-implanted 6H-SiC after 1400 °C/10 min annealing.

behavior of the persistent (divacancy) D_1 centers is considered as a possible reason for poor acceptor activation in SiC.[39]

D. Electrical characterization

In the as-implanted material the implant is predominantly in the interstitial sites of the lattice. For electrical activation the implant should be driven into the lattice (substitutional) sites during annealing. During chemical vapor deposition by varying Si/C ratio in the reactor, Larkin *et al.*[40] proved that Al takes Si lattice sites in SiC. The results of x-ray diffraction have also indicated that Al in SiC occupies only the silicon sites.[41,42] But at this time there is no clear understanding of B incorporation in SiC. There are a few reports,[43,44] which suggest that B occupies mainly the Si lattice sites in SiC and the B_{Si} acceptor has an activation energy of 0.38 eV.[45] Some of the B atoms can also occupy the C sites and the degree of B_C concentration depends on growth method and doping conditions.[46] The B_C acceptor has an activation energy of 0.6–0.7 eV.[46] According to Konstantinov[46] in the diffused profiles B predominantly occupies Si sites at the surface and C sites at the tail.

We have made van der Pauw Hall and C-V profiling measurements on implanted and annealed material to obtain carrier (hole) concentration and carrier mobility. For van der Pauw Hall measurements, Al/Ti alloyed ohmic contacts were used, whereas for C-V measurements Al Schottky metal contacts were formed. All 6H- and 3C-SiC samples implanted with Al or B at room temperature and with B at 850 °C showed n-type behavior after annealing. Similar behavior is observed for 850 °C Al-implanted 3C-SiC annealed at 1200 °C and 6H-SiC annealed at 1100 °C. In all the above samples the residual implant damage is high due to room temperature implantation and/or low annealing temperatures. We observed p-type behavior in 850 °C Al-implanted samples annealed at 1400 °C. This behavior was confirmed by both Hall and C-V profiling measurements. These measurements indicated an activation of ~1% which corresponds to a peak hole concentration of 5×10^{17} cm^{-3}. The measured hole mobility is 30–40 cm^2/V s.

Poor implant acceptor activation is one of the stumbling blocks in developing ion implantation technology for SiC device processing. This could be due to (1) complexing of the acceptor implant with Si or C or with C or Si vacancies created during the implantation/annealing process, (2) the implant species residing on non-electrically active interstitial sites, (3) the presence of thermally stable deep donor type defects in the implantation layer,[6,9] or (4) trapping of impurities at the dislocations and stacking faults in the material.[2]

Presently we are in the process of investigating coimplantation of Al and B acceptors with C or Si in 6H-SiC. Coimplantation of one of the substrate constituent species decreases vacancies in like sites and increases vacancies of the other constituent element. If poor activation is indeed due to complexing of the dopant with vacancies of one of the substrate elements the coimplantation technique will suppress the complexing. In SiC the formation energy of a carbon vacancy (V_C) is relatively low (4.0 eV) and V_C acts as a double donor.[47] If the donor compensation behavior of V_C is responsible for poor acceptor activation, C coimplantation will help reduce the V_C concentration. In addition, since C coimplantation creates silicon vacancies (V_{Si}) the acceptor activation can be improved too. It is known that Al takes Si lattice sites to act as an acceptor. Since the formation energy of V_{Si} is 7.8 eV,[47] the V_{Si} concentration is probably too low compared to V_C (without C coimplantation) to yield good acceptor activation. By using the coimplantation technique, higher electrical activation was obtained for donor implants in GaAs[48] and acceptor implants in InP.[49,50]

IV. CONCLUSIONS

In conclusion, Al and B implantations were performed into n-type 6H- and 3C-SiC at RT and 850 °C and the material was annealed at 1100–1400 °C for 10 min. P-type conduction was observed only in samples implanted by Al at 850 °C and annealed at 1400 °C. For the remaining implant/anneal conditions the material remained n-type. After 1400 °C annealing, the implant was gettered at the 0.7 R_p location where the lattice damage is maximum. Only a slight in-diffusion of the implant was observed for the annealing conditions used in this study. The samples implanted at

850 °C were not amorphized and RBS yields close to the virgin level were obtained after 1400 °C annealing. For the samples implanted at RT, the as implanted damage was close to the random level and a distinct damage peak remained in the RBS spectrum even after 1400 °C annealing. Implant-damage-related peaks were seen in the photoluminescence spectrum recorded on elevated temperature Al and B implanted 6H- and 3C-SiC and no donor-acceptor pair transitions were seen even after 1400 °C annealing, indicating a poor implant activation. Currently we are investigating C and Si coimplantations along with the B and Al to improve the implant acceptor activation.

ACKNOWLEDGMENTS

We thank J. Kretchmer for his help during the course of this study. The work at George Mason is supported by NSF under grant # ECS-9319885 and the work at ORNL is supported by Division of Materials Sciences, U.S. Department of Energy under contract No. DE-AC05-84OR21400 with Martin Marietta Energy Systems, Inc.

[1] N. W. Jepps and T. F. Page, in *Progress in Crystal Growth and Characterization*, edited by P. Krishna (Pergamon, New York, 1983), Vol. 7, p. 259.
[2] R. F. Davis, G. Kelner, M. Shur, J. W. Palmour, and J. A. Edmond, Proc. IEEE **79**, 677 (1991).
[3] P. Glasow, G. Ziegler, W. Suttrop, G. Pensl, and R. Helbig, in SPIE Conference Proceedings, Vol. 868, p. 40.
[4] J. W. Palmour, J. A. Edmond, H. S. Kong, and C. H. Carter, Jr., in Proceedings of the 7th Trieste Semiconductor Symposium–Wide Bandgap Semiconductors, edited by C. Van de Walle.
[5] H. L. Dunlap and O. J. Marsh, Appl. Phys. Lett. **115**, 311 (1969).
[6] O. J. Marsh and H. L. Dunlap, Rad. Eff. **6**, 301 (1970).
[7] O. J. Marsh, in *Silicon Carbide–1973*, edited by R. C. Marshal, J. W. Faust, Jr., and C. E. Ryan (University of South Carolina Press, Columbia, SC, 1974), p. 471.
[8] A. Addamiano, G. W. Anderson, J. Comas, H. L. Hughes, and W. Lucke, J. Electrochem. Soc. **119**, 1355 (1972).
[9] S. A. Belova, A. V. Vorob'ev, V. M. Gusev, K. D. Demakov, M. G. Kosaganova, N. K. Prokof'eva, M. B. Reifman, V. G. Stolyarova, and V. A. Uzhegova, Sov. Phys. Semicond. **10**, 743 (1976).
[10] E. E. Violin, K. D. Demakov, A. A. Kalnin, F. Nolbert, E. N. Potapov, and Yu. M. Tairov, Sov. Phys. Solid State **26**, 960 (1984).
[11] V. A. Gudkov, G. A. Krysov, and V. V. Makarov, Sov. Phys. Semicond. **18**, 684 (1984).
[12] E. V. Kalinina, A. V. Survov, and G. F. Kholuyanov, Sov. Phys. Semicond. **14**, 652 (1980).
[13] J. A. Edmond, H. J. Kim, and R. F. Davis, Materials Research Society Symposium Proceedings 52, p. 157.
[14] J. Ryu, H. J. Kim, and R. F. Davis, Ref. 13, p. 165.
[15] J. A. Edmond, S. P. Withrow, W. Wadlin, and R. F. Davis, Mater. Res. Soc. Symp. Proc. **77**, 193 (1987).
[16] G. Pensl, R. Helbig, H. Zhang, G. Ziegler, and P. Lanig, Mat. Res. Soc. Symp. Proc. **97**, 195 (1987).
[17] R. E. Avila, J. J. Kopanski, and C. D. Fung, J. Appl. Phys. **62**, 3469 (1987).
[18] K. K. Burdel, P. V. Varankin, V. N. Makarov, A. V. Suvorov, and N. G. Chechenin, Sov. Phys. Solid State **30**, 364 (1988).
[19] J. A. Edmond, K. Das, and R. F. Davis, J. Appl. Phys. **63**, 922 (1988).
[20] J. Ryu, H. J. Kim, J. T. Glass, and R. F. Davis, J. Electron. Mater. **18**, 157 (1989).
[21] M. Ghezzo, D. M. Brown, E. Downey, J. Kretchmer, W. Hennessy, D. L. Polla, and H. Bakhru, IEEE Electron. Device Lett. **13**, 639 (1992).
[22] M. Ghezzo, D. M. Brown, E. Downey, J. Kretchmer, and J. J. Kopanski, Appl. Phys. Lett. **63**, 1206 (1993).
[23] M. Ikeda, H. Matsunami, and T. Tanaka, Phys. Rev. B **22**, 2842 (1980).
[24] J. F. Ziegler, J. P. Biersack, and U. Littmark, *The Stopping and Range of Ions in Solids* (Pergamon, New York, 1985).
[25] J. Gyulai, in *Handbook of Ion Implantation Technology*, edited by J. F. Ziegler (North-Holland, New York, 1992), p. 106.
[26] L. A. Christel and J. F. Gibbons, J. Appl. Phys. **52**, 5050 (1981).
[27] R. E. Avila and C. D. Fung, J. Appl. Phys. **60**, 1602 (1986).
[28] W. Lucke, J. Comas, G. Hubler, and K. Dunning, J. Appl. Phys. **46**, 994 (1975).
[29] S. G. Roberts and T. F. Page, J. Mater. Sci. **21**, 457 (1986).
[30] H. G. Bohn, J. M. Williams, C. J. McHargue, and G. M. Begun, J. Mater. Res. **2**, 107 (1987).
[31] J. A. Edmond, S. P. Withrow, H. S. Kong, and R. F. Davis, Mater. Res. Soc. Symp. Proc. **51**, 395 (1986).
[32] J. A. Freitas, Jr., S. G. Bishop, J. A. Edmond, J. Ryu, and R. F. Davis, J. Appl. Phys. **61**, 2011 (1987).
[33] G. Pensl and R. Helbig, Festkrperprobleme **30**, 133 (1990).
[34] W. J. Choyke, Z. C. Fong, and J. A. Powell, J. Appl. Phys. **64**, 3163 (1988).
[35] J. A. Freitas, Jr. and S. G. Bishop, Appl. Phys. Lett. **55**, 2757 (1989).
[36] W. J. Choyke, Inst. Phys. Conf. Ser. **31**, 58 (1977).
[37] W. J. Choyke and L. Patrick, Review of Optical Work in SiC since 1968, p. 261.
[38] P. A. Glasow, in *Amorphous and Crystalline Silicon Carbide*, edited by G. L. Harris and C. Y.-W. Yang (Springer, Berlin, 1989), p. 23.
[39] L. Patrick and W. J. Choykee, Phys. Rev. B **5**, 3253 (1972).
[40] D. J. Larkin, P. G. Neudeck, J. A. Powell, and L. G. Matus, Inst. Phys. Conf. Ser. **137**, 51 (1994).
[41] S. Yamada and H. Kuwabara, *Silicon Carbide-73*, Proc. Third Intern. Conf., Miami Beach, FL, 1973, edited by R. C. Marshal, J. W. Faust, Jr., and C. E. Ryan (University of South Carolina Press, Columbia, SC, 1974), p. 305.
[42] U. Hagen and A. W. C. Van Kamenade, Phys. Status Solidi A **33**, 97 (1976).
[43] R. N. Kyutt, E. N. Mokhov, and A. S. Tregubova, Sov. Phys. Solid State **23**, 2034 (1981).
[44] A. G. Zubatov, I. M. Zaritskii, S. N. Lukin, E. N. Mokhov, and V. G. Stepanov, Sov. Phys. Solid State **27**, 197 (1985).
[45] Yu. A. Vadakov, N. Zhumaev, B. P. Zverev, G. A. Lomakina, E. N. Mokhov, V. G. Oding, V. V. Semenov, and Yu. F. Simakhin, Sov. Phys. Semicond. **11**, 214 (1977).
[46] A. O. Konstantinov, Sov. Phys. Semicond. **26**, 151 (1992), and the references therein.
[47] C. Wang, J. Bernholc, and R. F. Davis, Phys. Rev. B **38**, 12 752 (1988); Mater. Res. Soc. Symp. Proc. (1990).
[48] K. K. Patel and B. J. Sealy, Appl. Phys. Lett. **48**, 1467 (1987).
[49] K-W. Wang, Appl. Phys. Lett. **51**, 2127 (1987).
[50] M. V. Rao and R. K. Nadella, J. Appl. Phys. **67**, 1761 (1990).
[51] Certain commercial materials are identified in this paper in order to specify adequately the experimental procedure. Such identification does not imply that the materials identified are necessarily the best available for the purpose.